

An Improvement VSC-HVDC Station in Thailand

Narin Watanakul

Thammasat University of Thailand, Faculty of Engineering, Department of Electrical and Computer Engineering, Rangsit Campus, Klong Luang, Pathumthani, Thailand.
E-mail:wnarin@engr.tu.ac.th

Abstract— The paper was to study design and improvement voltage source converter (VSC) based HVDC long-distance transmission system around 110km between Thailand to Malaysia with rated 300MVA (± 300 kV). This paper presents an application of an asynchronous back to back VSC-HVDC system, which uses multilevel converter a 7-level Diode-Clamped SPWM converters topology technique for the realization of HVDC system. The controller has been proposed by using PQ control and feed-forward decoupled current control algorithm. The design and experimentally controllers of VSC in lab scaled test, MATLAB/Simulink program were performed VSC-HVDC transmission system, simulation in order to evaluate transient performance, can be controlled independently under two phase to ground faulted and three phases to ground faulted conditions. The system are used as a guideline for analysing and design of the data process control with the PQ-control HVDC system.

Keyword- Voltage direct current (HVDC), Voltage source converter (VSC), multilevel converter (MC), Phase level shift, PQ control, Diode-Clamped SPWM converters.

I. INTRODUCTION

Electrical energy is normally transmitted by means of transmission line. An electric circuit is an interconnection of electrical elements connected together in a closed path so that an electric current may flow continuously. Transmission by ac replaced dc transmission because of the case and efficiency with which voltage can be transformed using transformers. The disadvantage of AC transitions system, the volume of copper used is much more than the D.C. system, the inductance and capacitance of the line effects the regulation of the line which is increased due to skin effect the line resistance is increased which further increases the skin effect, the AC transmission lines are more effective to corona than D.C. lines, in an A.C. system the speed of the generator and alternators is not economical, variation of these speeds must be controlled within very low limits, in cable the alternating current cause sheath loss. The construction of the transmissions lines is not so easy as in case of D.C. lines, the alternator must be synchronized, before they are made to run in parallel. The factor of limitation of AC transitions system for long-distance transitions consist of voltage stability, reactive power problems, steady-state stability and transient stability. For interconnected of AC transitions system consist of load-flow problems (management of congestion), frequency control, voltage stability, inter-area oscillation and blackout risk due to cascading effects. For example HVDC of Thailand and Malaysia installed in June 2002. The HVDC Thailand–Malaysia is a 110 kilometre long HVDC power line between Khlong Ngae in Thailand at $6^{\circ}42'56''\text{N } 100^{\circ}27'08''\text{E}$ and Gurun in Malaysia. The HVDC Thailand–Malaysia, which crosses the border between Malaysia and Thailand at $6^{\circ}31'47''\text{N } 100^{\circ}24'11''\text{E}$, serves for the coupling of the asynchronously operated power grids. The HVDC connection Thailand–Malaysia is a monopoles 300 kV DC overhead line with a maximum transmission rate of 300 megawatts (MW). The terminal of the HVDC is situated east of Gurun at $5^{\circ}48'45''\text{N } 100^{\circ}32'06''\text{E}$ as shown in Fig.1(a). This HVDC long-distance transmission system interconnecting the 230 kV AC network of Thailand with the 275 kV AC network of Malaysia is implemented in the first stage as a 300 MW monopoles metallic return scheme as shown in figure (Fig.1(b)).

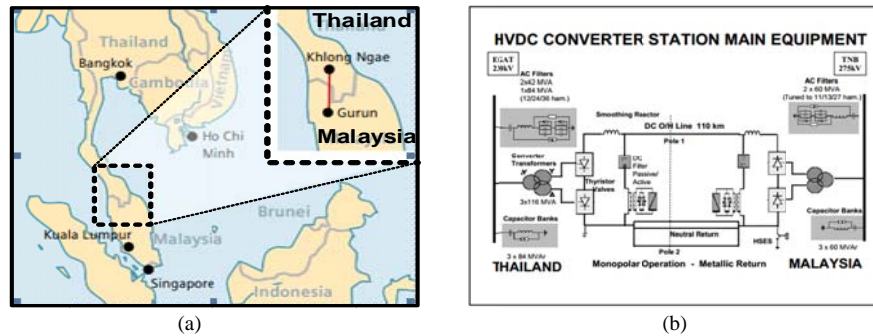


Fig.1. (a) The Map on location of this HVDC long-distance transmission system between interconnecting the 230 kV AC network of Thailand with the 275 kV AC network of Malaysia (b) Typical schematic of distribution power system with HVDC converter station main equipment

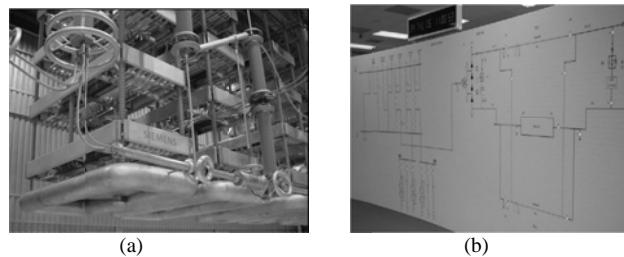


Fig. 2. The components of HVDC has been installed for current user (a) Components of HVDC Type of thyristor Electrically-triggered-thyristor, 8kV (100 mmØ) and (b) single line diagram of Monopoles links HVDC system configurations and components.

In present of installed monopoles link HVDC system configurations and components in Thailand consist of AC switchgear, and the interconnecting 300 kV DC overhead line was included in Siemens' scope of supply. Commercial operation started in 2001. Technical Data Customer Electricity Generating Authority of Thailand (EGAT) Tenaga Nasional Berhad (TNB) Project name Thailand–Malaysia Location Khlong Ngae–Gurun Power rating 300 MW, monopoles Type of plant Long-distance transmission, 110 km Voltage levels 300 kVdc, EGAT: 230 kV, 50 Hz TNB: 275 kV, 50 Hz Type of thyristor Electrically-triggered-thyristor, 8 kV (100 mm Ø) [1],[2] as show in Fig.2 (a)-(b). Environmental constraints will play an important role in the power system developments [3],[4]. However, regarding the system security, have to be integrated into the system, particularly when the connecting AC links are weak and when sufficient reserve capacity in the neighbouring systems is not available [5]. In the future, an increasing part of the installed capacity will be connected to the distribution levels (dispersed generation), which poses additional challenges to the planning and safe operation of the systems. Power electronics will be required to control load flow, to reduce transmission losses and to avoid congestion, loop flows and voltage problems [6]–[7]. Basically, there are three kinds of multilevel inverters. The multilevel converter topology for the VSC transmission system consist of the cascade converters (CC), flying capacitor converter (FC) and neutral point clamped SPWM converter (NPC) [8]. The comparison between VSC HVdc transmission and LCC transmission. The LCC that the reverse voltage is available only for a 180° interval from the firing angle $\alpha=0^\circ$ point of the conducting thyristor. Due to the inductance in series with the ac voltage, this process takes a certain amount of time – corresponding to the overlap angle. If the firing of this next valve is delayed too much, the commutation (transfer of current from outgoing valve to incoming valve) is not successful and this phenomenon is referred to as commutation failure. Dependence on an ac voltage source, Reactive power consumption or generation requirement for ac system. For LCC HVdc consumes reactive power of 50% to 60% of the active power. Switchable shunt capacitor banks are necessary for reactive power compensation. For VSC HVdc transmission, the dc side voltage in a VSC is essentially kept constant. A VSC system instead can keep the same voltage polarity for power reversal. The same voltage polarity during power reversal makes the dc grid possible. For reactive power can be generated or absorbed. Reactive power can be controlled independently from active power control at both ends of the VSC Transmission scheme.

This article presents application diagram of voltage source converter (VSC) station in Thailand to Malaysia with control of an asynchronous back to back VSC-HVDC system, which uses 7-level neutral point clamped SPWM converter topology technique, and a feed-forward decoupled current control in rotation frame that the ac current is decoupled algorithm. The process PQ controller can realize the designated control of active power (P) and reactive power (Q) strategy. the PQ power can exchange controlled independently, The simulation results got from MATLAB software confirm that the control strategy provides satisfactory response and strong stability.

II. BACK-TO BACK DIODE-CLAMPED CONVERTER SYSTEM

Basically, Three-level diode-clamped converter/inverter [9]. The neutral point converter proposed by Nabae, Takahashi, and Akagi in 1981 was essentially a In the 1990 several researchers published articles that have reported experimental results for four-, five-, and six-level diode-clamped converters for such uses as static var compensation, variable speed motor drives high voltage, and high voltage system interconnections [10-13]. A three-phase seven-level diode-clamped converter as shown in Fig.3.

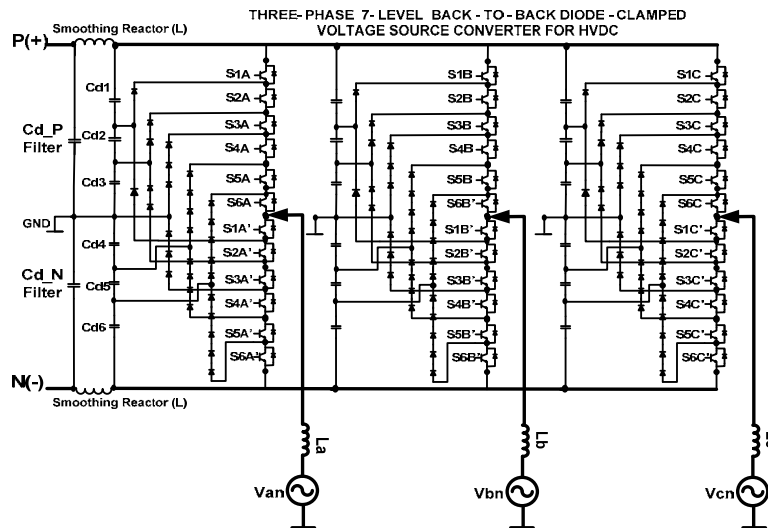


Fig. 3. three-phase seven-level diode-clamped converter circuit diagram.

As shows in Fig.3. The number of clamping diodes increases substantially with the voltage level VSC station system, for example 7 - level voltage, the number of IGBT required for circuit system will be $6(m-1)$ about 36 IGBT set, the number of diode required for circuit will be $3(m-1).(m-2)$ about diodes are using 90 set (Power diode) and , the number of capacitor required the dc capacitor it means equation $(m-1)$ about 6 capacitor per phase (Cdc1-Cdc6). Each of the three phases of the converter shares a common dc bus, which has been subdivided by six capacitors into seven levels. The voltage across each capacitor is V_{dc} , and the voltage stress across each switching device is limited to V_{dc} through the clamping diodes. Table 1.1 illustrated lists the output voltage levels possible for one phase of 7-level diode-clamped converter using the negative dc rail voltage V_0 as a reference. State condition “1” means the switch is on, and “0” means the switch is off. Note phase has seven complementary switch pairs such that turning on one of the switches of the pair requires that the other switch be turned off. The complementary switch pairs for phase leg a are (Sa1 Sa’1), (Sa2, Sa’2), (Sa3, Sa’3), (Sa4, Sa’4), (Sa5, Sa’5) and (Sa6, Sa’6). For a 7-level converter, a set of six switches is on at any given time. Advantages for all the phases share a common dc bus, which minimizes the capacitance requirements of the converter. For this reason, a back-to-back topology is not only possible but also practical for uses such as a high-voltage back-to-back inter-connection. The capacitors can be pre-charged as a group. Efficiency is high for fundamental frequency switching. For disadvantages: Real power flow is difficult for a single inverter because the intermediate DC levels will tend to overcharge or discharge without precise monitoring and control. The number of clamping diodes required is quadratic ally related to the number of levels, which can be cumbersome for units with a high number of levels [10],[11].

TABLE I

Diode-Clamp 7-level Converter Voltage Levels and corresponding switch states
 “1” means the switch is on, and “0” means the switch is off.

Output(Vab)	Switch State											
	Sa6	Sa5	Sa4	Sa3	Sa2	Sa1	Sa6'	Sa5'	Sa4'	Sa3'	Sa2'	Sa1'
V7 = 6Vdc	1	1	1	1	1	1	0	0	0	0	0	0
V6 = 5Vdc	0	1	1	1	1	1	1	0	0	0	0	0
V5 = 4Vdc	0	0	1	1	1	1	1	1	0	0	0	0
V4 = 3Vdc	0	0	0	1	1	1	1	1	1	0	0	0
V3 = 2Vdc	0	0	0	0	1	1	1	1	1	1	0	0
V2 = Vdc	0	0	0	0	0	1	1	1	1	1	1	0
V1 = 0	0	0	0	0	0	0	1	1	1	1	1	1

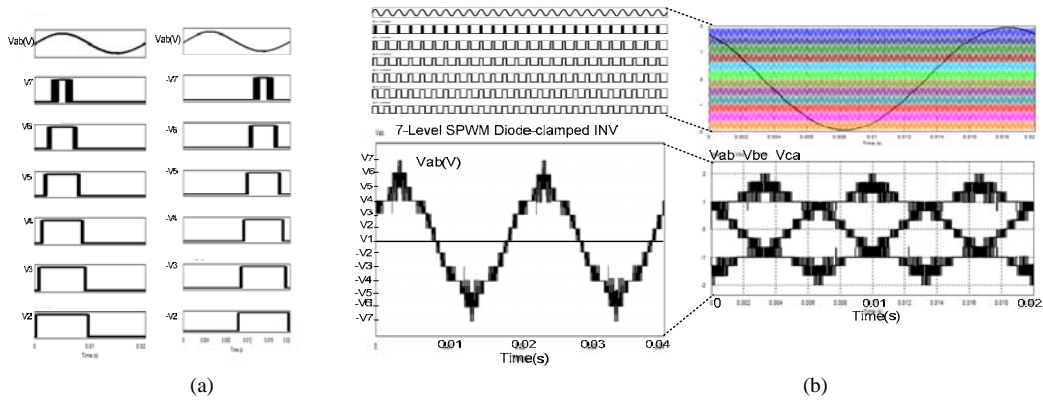


Fig. 4. (a) The timing diagram of gate voltage waveforms for driver (b) voltage waveform resulting line-line voltages (Vab) corresponding for seven-level diode-clamped converter.

As shown in figure (Fig.4 (a) and Fig(b)) illustrate that the smallest distortion is obtained of multilevel SPWM with modulation ($m_a = 1$) by phase level shifted carriers angle 45 deg for seven-level SPWM with carrier-based PWM techniques and designs setting switching frequency ($f_s=10\text{kHz}$). The line-line voltage is an 13-level staircase waveform voltage, this means that an m-level diode-clamped converter has an m-level output phase voltage and a $(2m-1)$ level output line voltage. The line voltage consists of a positive and negative phase-leg ($a-b$) voltages about ($V_{ab} = V_{a1}+V_{a2}+v_{a3}+v_{a4}+V_{a5}+V_{a6}+V_{a7}$) [14].

III. VOLTAGE SOURCE CONVERTER BASED HVDC TRANSMISSION

As schematically shown in Fig. 5 shows the circuit diagram configuration of a proposed voltage source converter (VSC) interconnection between from Thailand station (1) to Malaysia (2) station with control of an asynchronous back to back VSC-HVDC system, each station(1) and (2) rated 300MW(+/-300kV DC), which uses 7-level SPWM converter topology. The sending and receiving VSC station have same topology structure. The AC system in Thailand station converter is rated at $3 \times 116\text{MVA}, 230\text{kV}/122.24\text{kV}/822\text{A}/50\text{Hz}$, and Malaysia station converter is rated about at $3 \times 116\text{MVA}, 275\text{kV}/122.24\text{kV}/822\text{A}/50\text{Hz}$. The rectifier and the inverter are interconnected through a 110km cable (i.e. 2 pi section) and DC filter connected smoothing reactor (L) and capacitor ($C1=C2$). The two terminals are interconnected by a DC link. Each station consist of phase-shift transformer winding, transformer with two separated winding (delta and wye) one wye primary winding and two secondary winding (Δ/Y), similar to a 12-pulse rectifier system, cancellation of the 5th and 7th can be achieved on the primary side of the transformer to the degree that these currents are balanced in each of the transformer secondary windings, illustrate current waveform simulation by MATLAB as shown in figure (Fig.6).

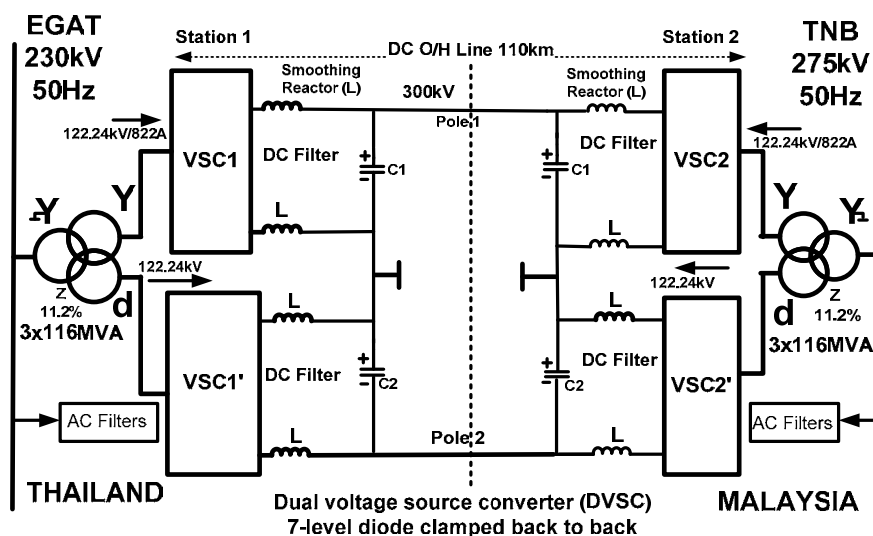


Fig. 5. The two-terminal VSC system, Voltage Source Converter (VSC) Based HVDC Transmission system configuration.

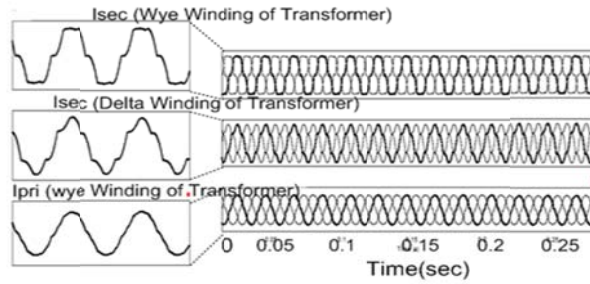


Fig. 6. Current of transformer for wye primary winding and two secondary winding (Δ / Y) with phase-shift transformer.

We apply Kirchoff's voltage Law (KVL) is deduction of the power static equations with power delivered to the stiff grid. Expressing complex power Eq(3), and as shown single line diagram of equivalent circuit of power flow as shown in figure (Fig.7.).

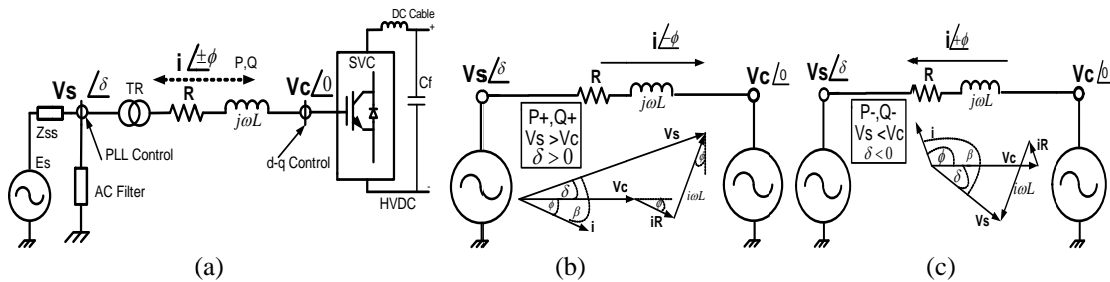


Fig. 7. Phasor diagram and the single line diagram of inductance (WL) and resistance (R), the total impedance coming from transformer and phase reactor, point (Vs) is the PCC of the grid ac system, Point (Vc) is the voltage source converter (VSC), (a) A typical configuration of a VSC converter terminal (b) active and reactive power flows (P+ and Q+) and (c) active and reactive power flow (P- and Q-).

IV. MODELLING CONTROLLER FOR 7-LEVEL DIODE-CLAMPED INVERTER

This paper describes the operation and control of the VSC based HVDC transmission system has been proposed using by Direct Power Control (PQ) controlled multilevel voltage source converter with 7-level SPWM. The modelling block diagram consists of PLL (phase Lock Loop) used control with the line voltages and also to compute the transformation angle used in the *d* and *q*-axis, using by the sine-cosine-ROM is vital for in-phase strategy controller wave form. We obtain current (*Ia, Ib, Ic*) and voltage (*Va, Vb, Vc*) it is that flow pass LPF is 1st-order low-pass filter that LPF (low- Pass Filter) frequency signals setting of design Cut-off frequency ($f_c=1000\text{Hz}$).

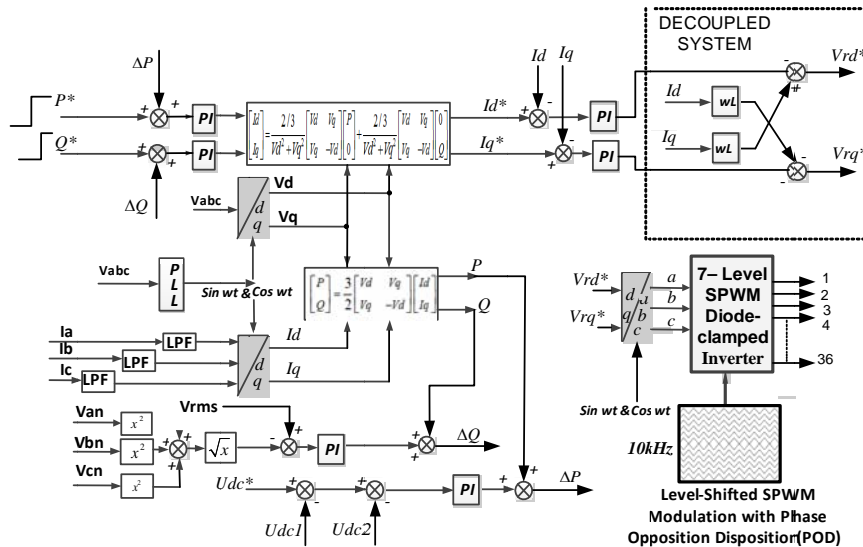


Fig. 8. Modelling directed power control for multilevel voltage source converter with 7-level Diode-Clamped SPWM converter topology

In equation Eq(1), gives that active power (P) is proportional to the DC current and DC voltage. Furthermore it is mainly determined by the phase-displacement angle (δ). A positive phase-shift results in that the active power flows from the AC network to the converter. However the reactive power is mainly determined by the difference between the magnitudes of magnitudes of the AC bus voltage and the converter output voltage as shown in figure (Fig.7(a)) according to the Eq (1). The reactive power (Q) is fed from the voltage with higher magnitude towards the voltage with the lower magnitude. In equation Eq (2) - Eq (3), obtain current ($I\alpha, I\beta$) in the stationary reference frame (α, β), and transform to d-q transformation block current (I_d, I_q) and voltage (V_d, V_q) [15]. The decoupled system (Inner-controller) consist fo two axis id-command and iq-command components, in order to the performances of current PI-controllers in such system, cross-coupling terms current feed forward (i_d & i_q) as shown in figure (Fig.8). The PQ- theory power components are then calculated from voltages and currents in the value of dq-coordinates by using coordinates transformation. In this with the concept of d-q transformations in mind, we will discuss the mathematical representation of Single-line representation of voltages source converter (VSC). PQ-calculated, mean value of the instantaneous real power (P). It corresponds to the energy per time unity that is transferred from the power source to the load, in a balanced way, through the $a-b-c$ coordinates (it is, indeed, the only desired power component to be supplied by the power source). It is also important to note that the three-phase instantaneous power (P) can be written in coordinates systems, $a-b-c$ and dq- coordinates transform. Mean value of instantaneous imaginary power (Q), has to dq with power (and corresponding undesirable currents) that is exchanged between the system phases, and which does not imply any transference or exchange of energy between the power source and the load, can be written in both coordinates systems, $a-b-c$ and dq- coordinates transform, in $a-b-c$ coordinates the following expression is obtained the three-phase power source voltage can be easily as shows in equation Eq (4). In addition, in equation Eq (5), Eq (6), Eq (7) shows that there exist coupling between two axis components, however, the PI current controllers have no satisfactory tracking performance when they have to regulate coupled systems. Therefore, in order to improve the performances of the PI current controllers in such systems, cross-coupling terms (Inner (I_d & I_q) Controller) and current feed forward is usually convenient to used [8],[15],[16],[17],[18],[19],[20]. We get the steady fundamental component V_{an}, V_{bn}, V_{cn} by controllers proportional of V_{rd}^* and V_{rq}^* transformations voltage variation.

$$P = \frac{V_s V_c (R \cos \delta + \omega L \sin \delta) - V_c^2 R}{R^2 + \omega L^2}, \quad Q = \frac{V_s V_c (\omega L \cos \delta - R \sin \delta) - V_c^2 R}{R^2 + \omega L^2} \tag{1}$$

$$\begin{bmatrix} I\alpha(t) \\ I\beta(t) \end{bmatrix} = \sqrt{\frac{2}{3}} \begin{bmatrix} 1 & \cos \frac{2\pi}{3} & \cos \frac{4\pi}{3} \\ 0 & \sin \frac{2\pi}{3} & \sin \frac{4\pi}{3} \end{bmatrix} \begin{bmatrix} I_a(t) \\ I_b(t) \\ I_c(t) \end{bmatrix}, \quad \begin{bmatrix} V\alpha(t) \\ V\beta(t) \end{bmatrix} = \sqrt{\frac{2}{3}} \begin{bmatrix} 1 & \cos \frac{2\pi}{3} & \cos \frac{4\pi}{3} \\ 0 & \sin \frac{2\pi}{3} & \sin \frac{4\pi}{3} \end{bmatrix} \begin{bmatrix} V_a(t) \\ V_b(t) \\ V_c(t) \end{bmatrix}, \quad \begin{bmatrix} I_d \\ I_q \end{bmatrix} = \begin{bmatrix} \cos \alpha t & \sin \alpha t \\ -\sin \alpha t & \cos \alpha t \end{bmatrix} \begin{bmatrix} I\alpha \\ I\beta \end{bmatrix} \tag{2}$$

$$\begin{bmatrix} V_d \\ V_q \end{bmatrix} = \begin{bmatrix} \cos \omega t & \sin \omega t \\ -\sin \omega t & \cos \omega t \end{bmatrix} \begin{bmatrix} V\alpha \\ V\beta \end{bmatrix}, \quad \begin{bmatrix} I_a(t) \\ I_b(t) \\ I_c(t) \end{bmatrix} = \sqrt{\frac{2}{3}} \begin{bmatrix} 1 & 0 \\ \cos \frac{2\pi}{3} & \sin \frac{2\pi}{3} \\ \cos \frac{4\pi}{3} & \sin \frac{4\pi}{3} \end{bmatrix} \begin{bmatrix} I\alpha(t) \\ I\beta(t) \end{bmatrix}, \quad \begin{bmatrix} V_a(t) \\ V_b(t) \\ V_c(t) \end{bmatrix} = \sqrt{\frac{2}{3}} \begin{bmatrix} 1 & 0 \\ \cos \frac{2\pi}{3} & \sin \frac{2\pi}{3} \\ \cos \frac{4\pi}{3} & \sin \frac{4\pi}{3} \end{bmatrix} \begin{bmatrix} V\alpha(t) \\ V\beta(t) \end{bmatrix} \tag{3}$$

$$\begin{bmatrix} P \\ Q \end{bmatrix} = \frac{3}{2} \begin{bmatrix} V_d & V_q \\ V_q & -V_d \end{bmatrix} \begin{bmatrix} I_d \\ I_q \end{bmatrix}, \quad \begin{bmatrix} I_d \\ I_q \end{bmatrix} = \frac{2/3}{V_d^2 + V_q^2} \begin{bmatrix} V_d & V_q \\ V_q & -V_d \end{bmatrix} \begin{bmatrix} P \\ Q \end{bmatrix} + \frac{2/3}{V_d^2 + V_q^2} \begin{bmatrix} V_d & V_q \\ V_q & -V_d \end{bmatrix} \begin{bmatrix} 0 \\ 0 \end{bmatrix} \tag{4}$$

$$L \frac{d}{dt} \begin{bmatrix} I_d \\ I_q \end{bmatrix} = \begin{bmatrix} V_{s,d} \\ V_{s,q} \end{bmatrix} - \begin{bmatrix} V_{c,d} \\ V_{c,q} \end{bmatrix} - R \begin{bmatrix} I_d \\ I_q \end{bmatrix} - \omega L \begin{bmatrix} 0 & 1 \\ -1 & 0 \end{bmatrix} \begin{bmatrix} I_d \\ I_q \end{bmatrix} \tag{5}$$

$$V_{rd}^* = - \left(kpd + \frac{kid}{S} \right) (id^* - id) + \omega Liq \tag{6}$$

$$V_{rq}^* = - \left(kpq + \frac{kiqu}{S} \right) (id^* - id) - \omega Lid \tag{7}$$

TABLE II
Main system parameters the tester experimental & simulation

	Parameter	Rated-Value	Per unit
Station 1 (Rectifier Side) Thailand	Grid line Voltage	230kV(Base)	1.0
	Frequency	50Hz(Base)	1.0
	Rated Power	348MVA(Base)	1.0

	SCC, Impedance TR (Z)	11.20%	-
	Phase Shift Transformer (Y/ Δ /Y)	3x116MVA/230kV/ 122.24kV/822A	-
Station 1 (Inverter Side) Malaysia	Grid line Voltage	275kV(Base)	1.19
	Frequency	50Hz(Base)	1.0
	Rated Power	348MVA(Base)	1.0
	SCC, Impedance TR (Z)	11.20%	-
	Phase Shift Transformer (Y/ Δ /Y)	3x3116MVA/230kV/ 122.24kV/822A	-
VSC 7-Level Diode-Clamped SPWM Converter	Rated Power	300MVA	0.86
	Switching frequency	10kHz	200
	Number of Phase level shift multi-carrier Waves for 7-level SPWM	12	-
	Phase level shift angle	45deg	-
	Power IGBT/Diode	1200A/1200V	-
	LC-Filter HVDC Voltage Output Reactor & Capacitor	L1,L2 = 1mH C1,C2 = 85uF	-
	HVDC Voltage Output	± 300 kVDC	1.3
Cable: 2400mm ² /1563 A/321.5kV	110km x2 cable (R=0.0139 Ω /km)	L = 0.159mH/km C = 23.1uF/km	-
Converter Reactor	Reactor	300uH	-
Power Control Active Power (P)	Kp(P), Ki(P)	8, 10	-
Power Control Reactive Power (Q)	Kp(Q), Ki(Q)	4, 10	-
Inner (Id) Control	Kp(id), Ki(id)	0.75, 100	-
Inner (Iq) Control	Kp(iq), Ki(iq)	0.75, 100	-
AC Voltage Control	Kp(vac), Ki(vac)	20, 10	-
Vdc Voltage Control	Kp(vdc), Ki(vdc)	20, 10	-

Table 1. describes main system parameters for the tester experimental and simulation by MATLAB Simulink with 7-level Diode-Clamped SPWM converter. The performance of proposed PQ-control with dq-axis (censoring), dq-axis(command) and dq-axis, the controller design the inner control loop in d-axis and q-axis control can be done independently. Tuning of PI controllers in the current loops approach is to use the axis decoupling by means of feed forward control loops must be turn, the PI controllers in the outer control loops must be tuned to achieve a reasonable crossover, by in case short duration time. The parameter form a table for setup for design and improvement voltages source converter for containing load rating of 300MW for interconnection between from Thailand (station1) to Malaysia (station2) station with control of an asynchronous back to back VSC-HVDC system.

V. STUDY RESULTS

The consideration AC side perturbations, given the converter1 at rectifier-side (station 1) and converter 2 at the inverter side (station 2) was the controller designs are identical. An asynchronous back-to-back HVDC link based on VSC converter rated at 348kVA (± 300 kVDC) employing 7-level Diode-Clamped SPWM converter hardware prototype as shown in figure Fig.9(a), Fig.9(b) and Fig.9(c), the PWM has been tested for amplitude with modulation index ($m_a = 0.5, 0.8$) with sine wave with multicarrier waves (phase level shift) for three phase seven level SPWM system. The MATLAB Simulink, In order to test the dynamic responses of the VSC-HVDC regulators, two test cases have been studied. AC side perturbation, A two phase to ground fault was first applied at $t = 0.2$ sec to 0.3 sec at station 1 (Thailand) in order to investigate the behaviour of VSC-HVDC during unbalance faults. A three-phase to ground fault (Interruption short duration time) is applied at station 2 (Malaysia) at time, $t = 0.45$ sec to 0.55 sec is decreased to 0.0 pu and recovers fast and successfully to 1.0 pu. As usually $t < 0.20$ sec, the system operates in normal conditions and at $t > 0.30$ sec, station 1 is de-energized to clear the fault and at $t > 0.55$ sec, station 2 is de-energized to clear the fault, as shown in figure (Fig.10)- (Fig.12).

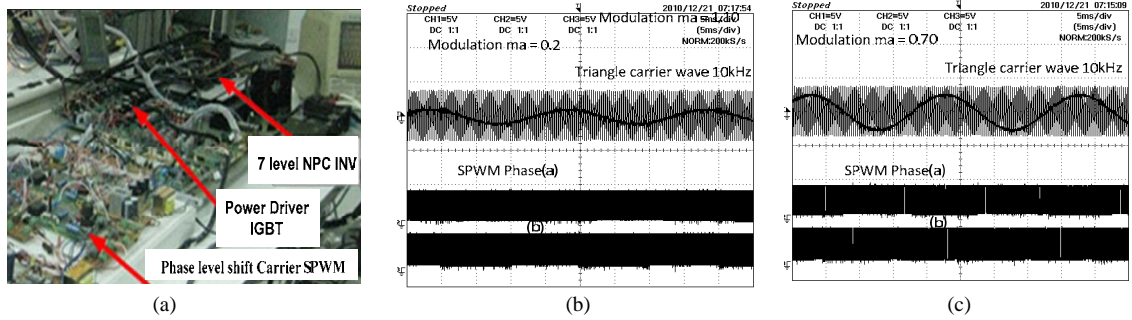


Fig. 9. Prototype of hard ware and SPWM Waveforms Sinusoidal pulse width modulation show, (a) Prototype of power drives 7-level SPWM converter of hard ware system (b) results of laboratory experiments test SPWM schemes is tested according to various control strategies such as switching frequency (fsw) and modulation index ma (0.5) and (c) test checking modulation SPWM ma (0.8)

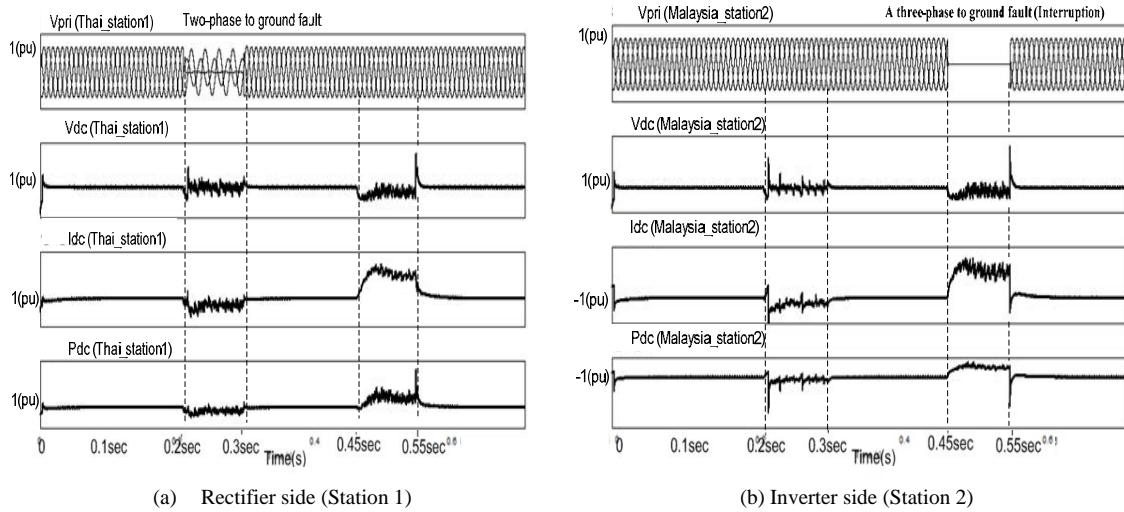


Fig. 10. MATLAB Simulation waveforms of the studied system under test case (a) a two-phase to ground fault at AC side perturbations in station 1 (Thailand) about DC voltage, DC current and DC power with short duration time start of period 0.20 – 0.30 second, we can see the DC voltages drops and it contains an oscillation during the fault. and (b) a three-phase to ground fault (Interruption short duration time) is applied at station 2 (Malaysia) at time, $t = 0.45 - 0.55$ second, it is consideration of the DC voltages drops an oscillation during the interruption fault.

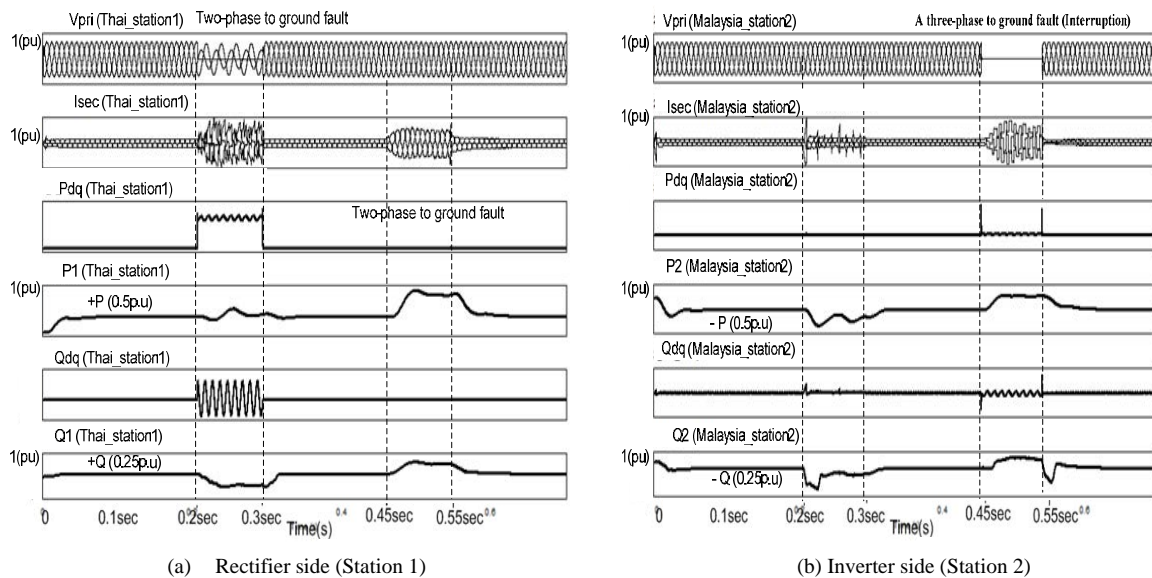


Fig. 11. MATLAB Simulation waveforms of the studied system as usually $t < 0.20$ sec power flow active power $+P(0.5p.u)$ and reactive power $+Q(0.25p.u)$ at station 1 (rectifier side), power flow active power $-P(0.5p.u)$ and reactive power $-Q(0.25p.u)$ at station 2 (inverter side) for the system operates in normal conditions and system under test case for fault condition (a) a two-phase to ground fault at AC side perturbations in station 1 (Thailand) about AC voltage (V_{pri}), AC current (I_{sec}), Pdq-coordinates, active power ($+P$) flow is $0.5p.u$,

transmitted from VSC1 to VSC2 at the rectifier side and oscillation Qdq-coordinates, reactive power (-Q) decreased 0.5 p.u. during the fault with short duration time start of period 0.20 – 0.30 second. and (b) a three-phase to ground fault (Interruption short duration time) is applied at station 2 (Malaysia) at time, $t = 0.45 - 0.55$ second, at $t > 0.55$ sec, station 2 is de-energized to clear the fault.

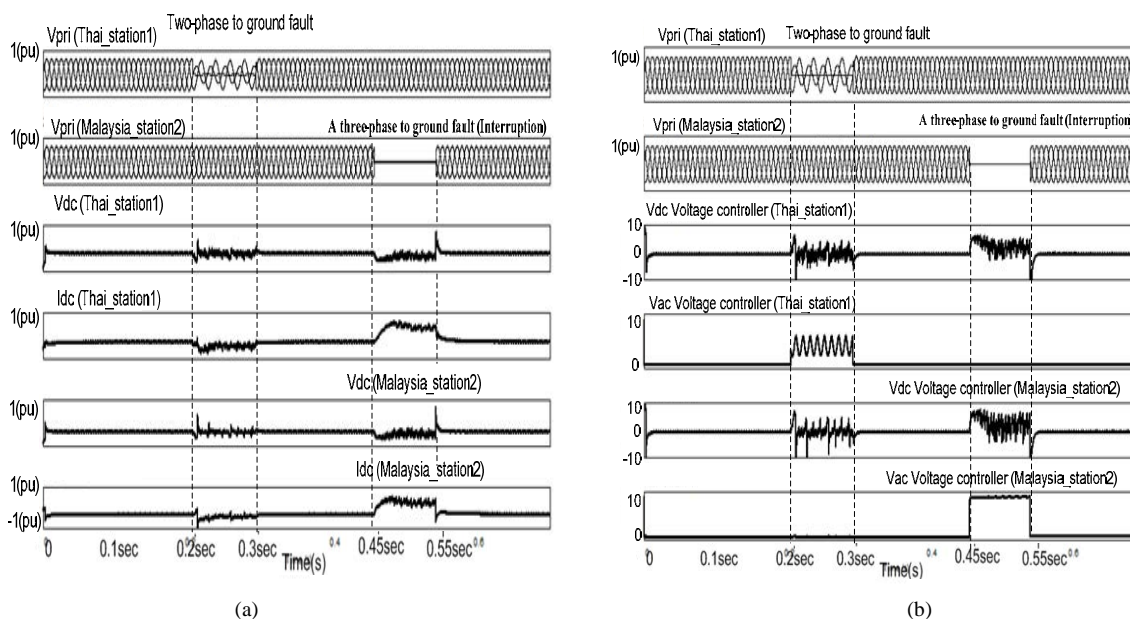


Fig. 12. MATLAB Simulation waveforms of the studied system under test case (a) a two-phase to ground fault with short duration time start of period 0.20 – 0.30 second and at three-phase to ground fault (Interruption short duration time) at time, $t = 0.45 - 0.55$ second of AC side perturbations in station 1 (Thailand) and at station 2 (Malaysia) about real time value of AC voltage (Vpri), DC voltage and DC current and (b) Vdc Voltage Controller and AC voltages controller for performance testing case of AC side perturbations with signal error compensated.

VI. CONCLUSION

In this paper, we have presents a control strategy of PQ-control to the multilevel converter (MC) with the phase level shift algorithm for 7-level Diode-Clamped SPWM converters topology technique for the realization of HVDC system. The feed-forward decoupled current control algorithm (inner control loop) in d-axis and q-axis control can be done independently. Tuning of PI controllers in the current loops approach is to use the axis decoupling by means of feed forward control loops must be turn. The power flows that the active power (P) and reactive power (Q) can be controlled with no mutual interference. In addition, the performance of the VSC-HVDC from the simulation, it can fulfil fast and bi-directional power transfers was verified by fault condition (one to two phase to ground fault and three-phase to ground fault (Interruption short duration time), when the fault is cleared, normal operation is recovered fast. This study also provides guideline to further analyse. In the future, simulations should be carried out to identify the appropriateness of the controllers.

REFERENCES

- [1] HVDC High Voltage Direct Current Transmission Unrivaled practical experience, www.siemens.com/energy/hvdc, <http://en.wikipedia.org>, <http://en.wikipedia.org>.
- [2] M. Davies, M. Dommaschk, J. Dorn, J. Lang, D. Retzmann, D. Soerangr, HVDC PLUS – Basics and Principle of Operation, <http://www.energy.siemens.com/br/pool/br/transmissao-de-energia/transformadores/hvdc-plus-basics-and-principle-of-operation.pdf>
- [3] European Technology Platform SmartGrids – Vision and Strategy for Europe’s Electricity Networks of the Future,” 2006, Luxembourg, Belgium.
- [4] DENA Study Part 1: “Energiewirtschaftliche Planung für die Netzintegration von Windenergie in Deutschland an Land und Offshore bis zum Jahr 2020,” February 24, 2005, Cologne, Germany.
- [5] M. Luther, U. Radtke, “Betrieb und Planung von Netzen mit hoher Windenergieeinspeisung,” ETG Kongress, October 23–24, 2001, Nuremberg, Germany
- [6] Economic Assessment of HVDC Links, CIGRE Brochure No.186 (Final Report of WG 14– 20)
- [7] N.G. Hingorani, “Flexible AC Transmission,” IEEE Spectrum, pp. 40–45, April 1993.
- [8] Mohamed Flitti *et al.* “Control of back-to-back voltage source converter,” Roum. Sci. Techn.– Électrotechn. et Énerg., 57, 3, p. 259–268, Bucarest, 2012.
- [9] A. Nabae, I. Takahashi, and H. Akagi, “A New Neutral-point Clamped PWM inverter,” IEEE Trans. Ind. Applicat., vol. IA-17, pp. 518–523, Sept./Oct. 1981.
- [10] L. M. Tolbert, F. Z. Peng, T. G. Habetler, “A Multilevel Converter-Based Universal Power Conditioner”, IEEE Transactions on Industry Applications, vol.36, no. 2, Mar./Apr. 2000, pp. 596-603.

- [11] L. M. Tolbert, F. Z. Peng, T. G.Habetler, "Multilevel Inverters for Electric Vehicle Applications," IEEE Workshop on Power Electronics in Transportation, Oct 22-23,1998, Dearborn, Michigan, pp. 1424-1431. 31-47.
- [12] F. Z. Peng, J. S. Lai, J. W.McKeever, J. VanCoevering, "A Multilevel Voltage-Source Inverter With Separate DC Sources for Static Var Generation," IEEE Transactions on Industry Applications, vol. 32, no. 5, Sept. 1996,pp. 1130-1138.
- [13] F. Z. Peng,J.S. Lai, "Dynamic Performance and Control of a StaticVar Generator Using Cascade Multilevel Inverters," IEEE Transactionson Industry Applications, vol. 33, no. 3,May 1997, pp.748-755.
- [14] J. S. Lai, F. Z. Peng, "Power converter options for power system compatible mass transit Systems," PCIM/Power Quality and Mass Transit Sys. Compatibility Conf., 1994, Dallas, Texas, pp. 285-294.
- [15] Khatir MOHAMED *et al.* "Performance Analysis of a Voltage Source Converter (VSC) based HVDC Transmission System under Faulted Conditions," Leonardo Journal of Sciences, Issue 15, July-December 2009, p. 33-46
- [16] Lindberg A.,ba Larsson T., "PWM and Contral of Three Level Voltage Sowrce Converters in an Hvdc Back-to-back Station," Sixth International Conference on AC and DC Power Transmission, 1996,pp.-297-302,29 Apr-3 May.
- [17] Lie Xu, Andersen B.R., Cartwright P., "Control of VSC transmission systems under unbalanced network conditions," Transmission and Distribution Conference and Exposition,7-12 Sept, 2003 IEEE PES, 2003, 2, pp.626-632.
- [18] M.khatir, S.A. Zidi, S. Hadijeri, M.K. Fellah, "Dynamic performance of back-to-back HVDC station based on voltage source converter," Journal of Electrical Engineering, 61,1, pp. 29-36 (2010).
- [19] Young-Min Parky, Han-Seong Ryu, Hyun-Won Lee, Myung-Gil Jung, and Se-Hyun Lee "Design of a Cascaded H-Bridge Multilevel Inverter Based on Power Electronics Building Blocks and Control for High Performance," Journal of Power Electronics, Vol. 10, May 2010.
- [20] Rokan Ali Ahmed, S. Mekhilef and Hew Wooi Ping, "New multilevel inverter topology with reduced number of switches," Proceedings of the 14th International Middle East Power Systems Conference (MEPCON'10), Cairo University, Egypt, December 19-21, 2010.

AUTHOR INFORMATION

Narin Watanakul graduated from the King Mongkut's of Technology North Bangkok, in Electrical Engineering (1986). He received Master University of Engineering degree (1993) from the same university. Currently, he is Associate Professor of the department of electrical and computer engineering, University. He is currently PhD at Faculty of Engineering Mahasarakham University (MSU), Thailand since 2008 respectively. His main research interests include power electronics, renewable energy converters and inverters, power quality, etc.